Diffusion MRI Tractography of Crossing Fibers by Cone-Beam ODF Regularization

H.H. Ehricke[1], K.M. Otto[1], V. Kumar[2], and U. Klose[2]

[1] Institute for Applied Computer Science, University of Applied Sciences, Stralsund, Germany

[2] Section of Experimental NMR of the CNS, University Hospitals, Tübingen, Germany

Abstract. Since the advent of high angular resolution diffusion imaging (HARDI) techniques in diffusion MRI great efforts have been taken in order to reconstruct complex white-matter structures, such as crossing, branching and kissing fibers. However, even highly sophisticated fiber tracking schemes, such as probabilistic tracking, suffer from the data's poor signal-to-noise (SNR) ratio. In this paper we present a novel regularization approach for q-ball fields, exploiting structural information within the data. We also propose a straightforward deterministic tracking algorithm, allowing delineation of even non-dominant pathways through crossing regions. Results from a phantom study with a biological phantom as well as a patient study, in which we reconstruct the pyramidal tract, emphasize the method's efficiency.

1 Introduction

In Magnetic Resonance Diffusion Imaging the diffusion tensor has been widely used as a model for the diffusion behavior of water molecules in a voxel. Streamline fiber tracking approaches on the basis of diffusion tensor imaging (DTI) have proven to yield good results for the reconstruction of dominant fiber structures within the brain white matter. However, for the delineation of more complex structures, such as kissing, crossing or branching fibers, clinically applicable techniques for image data acquisition and tracking are needed. Especially, for the tracking of non-dominant fiber populations, such as many sections of the optic, acoustic and pyramidal tracts, novel acquisition and processing schemes have to be elaborated which are capable of considering multiple fiber orientations in a voxel. Various imaging methods have been proposed in order to acquire a voxel's diffusion profile with far more than 60 gradient directions. Q-ball Imaging (QBI) and diffusion spectrum imaging (DSI) are two candidates in this category. Unfortunately, these high angular resolution diffusion imaging (HARDI) techniques have in common, that they are highly susceptible to artifacts, e.g. resulting from eddy currents or motion shift, and especially to noise. In QBI a model-independent reconstruction of the HARDI-Signal, leading to a diffusion orientation distribution function (ODF), is performed [1].

J. Denzler, G. Notni, and H. Süße (Eds.): DAGM 2009, LNCS 5748, pp. 412–421, 2009.

An ODF for a voxel at a discrete position (x_i, y_i, z_i) in 3D space may be imagined as a projection of diffusion probabilities p_{ij} onto the surface of a unit sphere, constructed around that voxel. Each diffusion probability p_{ij} corresponds to a discrete reconstruction point r_j on the unit sphere surface which can be defined by inclination/declination angles (ϕ_j, υ_j). For each of the reconstructed surface points r_j, its ODF value p_{ij} describes the diffusion probability in the direction $\overline{r_j}$, given by the unit vector from the sphere's center to the surface point. Thus we can describe an ODF as a discrete functional

$$\Psi_i(r_j) = p_{ij} \tag{1}$$

Due to symmetry reasons it is enough to distribute the datapoints r_j on a half-sphere: $\phi \in [0..2\pi], \upsilon \in [0..\pi]$.

If we interpret the probability value p_{ij} as a distance parameter, describing the datapoint's distance from the voxel center, we can transform the sphere model into a more complex shaped model, geometrically revealing the angular diffusion profile. The sharpness of this geometric representation is enhanced by normalization to the minimum to maximum interval, thus producing a min-max normalized ODF. However, the ODF's signal-to-noise ratio (SNR) typically is quite low, due to the restrictions of the imaging method. Therefore, an ODF usually is locally smoothed by applying a spherical convolution matrix. The kernel width defines the extent of a datapoint's neighborhood on the sphere in which samples contribute to smoothing. Especially in low-anisotropy regions of crossing and branching fibers this approach must be applied with great care, since it may suppress important details, e.g. signals stemming from non-dominant fibers.

During the last five years a variety of authors have proposed novel HARDI-based approaches, pursuing the idea of tracing pathways through areas of low diffusion anisotropy and thus allowing tracking of non-dominant pathways through crossing regions. Most of these techniques focus on tracking algorithms. Both, multiple-orientation deterministic methods as well as highly sophisticated and computationally expensive probabilistic techniques [2][3][4][5] have been designed. Most of them could improve the results for the delineation of specific brain regions with more complex white matter populations. Nevertheless, we are far from a general solution which would be clinically applicable.

2 Regularization of Diffusion MRI Datasets

In diffusion MRI the last decade has seen various approaches, most of them focused on DTI regularization. They fall into three categories, namely

1. regularization of diffusion weighted images prior to tensor reconstruction [6][7],
2. incorporation of a regularization scheme into the tensor estimation process [8],
3. regularization of tensor fields [9][10].

Most of these DTI-based approaches may not easily be transfered to HARDI-based imaging. Only a few novel techniques have been proposed for ODF regularization. Savadjiev et al. [11] model fibers by chains of helical segments. They use the notion of co-helicity in order to compute confidence values of ODF-directions of neighboring voxels. Three neighboring directions are co-helical if the direction vectors may be regarded as tangents of a helix segment, thus yielding a high confidence value for that direction. Summing up a direction's confidence values over the local neighborhood provides an estimate of local support. An iterative relaxation technique is used to maximize average local support. The drawbacks are computational expensiveness and the method's high complexity. For the latter reason parameter handling and interpretation of unwanted effects is not easy. Jonasson et al. [12] use ODF regularization prior to the segmentation of major white-matter tracts. They transfer the ODF dataset to a five-dimensional non-Euclidean position-orientation space (POS). Within this space they use an anisotropic diffusion filter with increasing number of iterations in order to produce multiple scales of resolution for the data. However, the spatial resolution and ODF sharpness is reduced with increasing degree of regularization and therefore it remains unclear, whether the approach might successfully be used in the framework of white-matter tractography. Descoteaux et al. [13] use spherical harmonics for ODF reconstruction. They incorporate a Laplace-Beltrami operator into the reconstruction scheme in order to sharpen the ODF. The operator reduces the influence of higher-order terms due to noise. The approach does not exploit the data from the voxel's local neighborhood, which certainly will limit its regularization effect when applied to real data. However, the method might be combined with regularization schemes, prior or after ODF reconstruction, such as our cone-beam regularization technique.

3 Cone-Beam ODF Regularization (CB-REG)

In signal processing noise-smoothing is a commonly used preprocessing step, necessary as a prerequisite for most signal analysis procedures. For QBI-based fiber tractography approaches smoothing of the ODF data is highly recommended, especially if more complex white matter structures are to be investigated. As explained above, ODF smoothing within a voxel [1][13] may lead to better tracking results, but by limiting the data source to the values, available within a voxel, the effect of the smoothing procedure is limited and the angular resolution is reduced. One way out of this dilemma is the incorporation of modeling assumptions into the smoothing procedure. E.g. Descoteaux et al. propose to transform the relatively unsharp and noisy diffusion-ODF into a sharper fiber-ODF by deconvolution with a diffusion-ODF kernel of a linear fiber model [14]. Another way, commonly used in image processing, is to operate on a local neighborhood, incorporating information from neighboring voxels into the process. With these local smoothing operators care has to be taken to avoid suppression of structural information, such as blurring of object edges. For this reason, more sophisticated smoothing approaches use structural information to steer the smoothing process. E.g. with anisotropic diffusion filtering [15] the intensity gradient magnitude is used to scale the filter function. Thus, smoothing over different objects is inhibited.

In the case of ODF de-noising our goal is to design a filter scheme which allows smoothing along fiber trajectories only. When we reduce noise, the ODF's shape becomes sharper and is more aligned with the underlying fiber architecture. Thus, the ODF field is regularized. In order to avoid smoothing over anisotropic regions with different diffusion orientations, we have to use structural information, given by the ODF function. In our CB-REG approach we apply smoothing to each datapoint p_{ij} on the ODF sphere at position (x_i, y_i, z_i) in 3D space. The datapoint's local neighborhood is defined by its direction vector $\overrightarrow{r_j}$ and two parameters α and l, describing opening angle and length of the cone-shaped neighborhood (fig. 1). The cone is centered around the direction vector $\overrightarrow{r_j}$ (cone A). Since the ODF is a symmetric function, a second cone B is constructed in the opposite direction $-\overrightarrow{r_j}$. Within each cone rays are sent along all direction vectors $\overrightarrow{r_k}$ encompassed by the cone shape: $\angle(\overrightarrow{r_k}, \overrightarrow{r_j}) \leq \frac{\alpha}{2}$. Each ray is then sampled by trilinear interpolation of ODFs at each unit step along the ray until the bottom of the cone has been reached. From each of the ODFs, sampled along a certain ray, only the datapoint, whose direction coincides with the ray direction is relevant. All relevant datapoints p_{mk} which have been sampled inside the cone are used in order to compute a smoothed ODF value $\tilde{\Psi}_i(r_j)$ by a weighted sum. We apply a two-dimensional Gaussian kernel $G(d, \delta)$ to scale each datapoint's weight according to its Euclidean distance $d_{mi} = \sqrt{(x_m - x_i)^2 + (y_m - y_i)^2 + (z_m - z_i)^2}$ from the cone center and the angle $\delta_{kj} = \angle(\overrightarrow{r_k}, \overrightarrow{r_j})$ between its direction $\overrightarrow{r_k}$ and the direction $\overrightarrow{r_j}$ around which the cone is centered . Thus the filtered ODF value $\tilde{\Psi}_i(r_j)$ is derived from the sampled ODF values $p_{mk} = \Psi_m(r_k)$ by:

$$\tilde{\Psi}_i(r_j) = \frac{1}{w} \sum_{m \in M, k \in K} G(d_{mi}, \delta_{kj}) \Psi_m(r_k) \tag{2}$$

where
M: set of sampled positions within cone A and cone B
K: set of sampled ray directions within cone A and cone B
w: sum of all weights of the sampled datapoints within cone A and cone B:

$$w = \sum_{m \in M, k \in K} G(d_{mi}, \delta_{kj}) \tag{3}$$

and

$$G(d, \delta) = e^{-\frac{d^2}{\sigma_d^2} - \frac{\delta^2}{\sigma_\delta^2}}. \tag{4}$$

The parameters σ_d and σ_δ define the sharpness of the two-dimensional Gaussian kernel. For simplification, we define a weight ω for the farthest distance $d = l$ and the widest angle $\delta = \frac{\alpha}{2}$ and compute σ_d and σ_δ such, that the utmost sample reaches a weight of ω.

In this manner we smooth only over a neighborhood of equal or similar diffusion directions, thus exploiting the structural information, given by the ODF itself. In the next chapter we explain, how we use the regularized q-ball field for tractography.

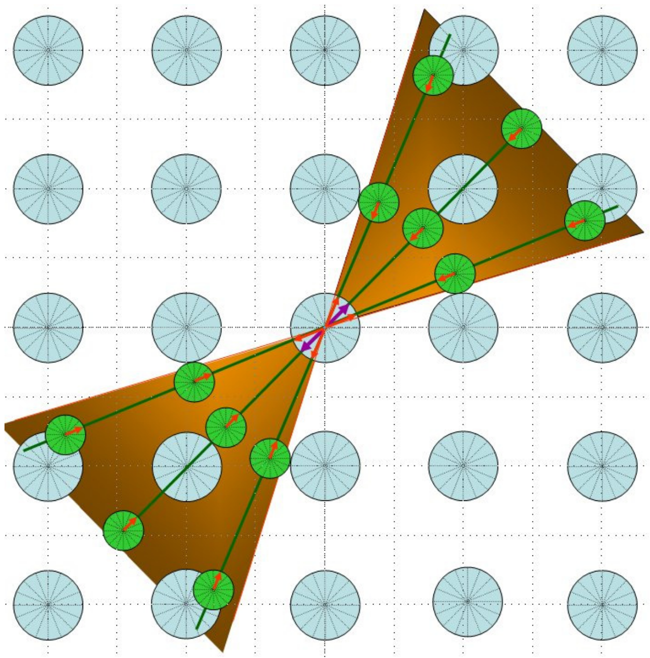

Fig. 1. Sketch of neighborhood sampling strategy used in cone-beam regularization, illustrating cone construction and sampling for a single ODF datapoint. Around the datapoint's direction and opposite direction (bold arrows) two cones are constructed. Within each cone ODFs are sampled (small circles) along direction rays by tri-linear interpolation within the ODF field (big circles). Only datapoints with directions along sampling rays are accepted (small arrows).

4 Deterministic ODF-Based Fiber Tracking

White matter tractography algorithms fall into two categories, deterministic and probabilistic. Deterministic approaches, such as streamline tracking [16] and tensor deflection (TEND) [17], integrate deterministic pathways using each sample's primary direction vector, typically derived from the diffusion tensor. Especially in more complex white matter regions estimated fiber directions contain a great amount of uncertainty, caused by noise, various artifacts and partial voluming. In these regions more sophisticated approaches are needed, e.g. dynamic fiber tracking which places secondary seeds in order to analyze connectivity of branching and crossing fibers [18]. With techniques from probability theory various authors have tried to improve tracking results. Most probabilistic tracking algorithms are based on an iterative Monte Carlo sampling scheme which is used to generate multiple trajectories from a seed point [2][19][3].

Perrin et al. are among the first to apply probabilistic fiber tracking to q-ball fields [20]. They propose a particle tracing approach where a particle entering a voxel with a certain speed and motion direction is deflected by a force, stemming from the local q-ball. The orientation of the force is chosen randomly inside a cone, defined from the incident direction. The ODF datapoints within the cone are used to control the random process. The main drawback of their approach is, that the reconstructed fibers diverge with increasing distance from the seed region. We have adapted their method to deterministic fiber tracking by substituting the random selection process. In our approach the trajectory direction we follow, is derived from the incident direction and the sample's ODF. We define a cone, centered around the incident direction. From the datapoints on the sphere only those, encompassed by the cone are taken into account. We select the tracking direction by determining the maximum ODF value within the cone. If the cone's maximum is less than 75 percent of the q-ball's overall maximum, we stop tracking, because the direction obviously does not represent anisotropic behavior. Otherwise, the direction vector of the maximum value is used for the next step of the integration process along the fiber pathway.

We use this straightforward algorithm because of its efficiency and its ability to track fibers through crossing regions, without being deflected by major pathways. Of course, the latter can only be achieved, if the ODFs in the q-ball field are sharp enough and their SNR is sufficiently high. Therefore, our deterministic fiber tracking algorithm is a good choice for the evaluation of regularization approaches.

5 Results

For evaluation of our regularization approach diffusion phantom data, provided by McGill University, Toronto was used. The phantom was constructed from excised rat spinal cord, embedded in agar in a configuration designed to have curved, straight and crossing tracts [21] (fig. 2). The q-ball data was acquired on a 1.5 Tesla Sonata MR scanner (Siemens, Erlangen) with 90 diffusion weighting directions, 30 slices and an isotropic resolution of 2.8 mm.

Fig. 2 shows the generalized fractional anisotropy (GFA) values from a slice through the phantom dataset (top left). The original ODFs are illustrated by the zoomed ODF shape display of the crossing region (top right). In the lower row results from ODF regularization with different parameters are displayed. In the left picture a cone length l of 2 voxels was used, whereas the right picture was produced with $l = 4$ voxels. In both cases a cone opening angle α of 30° and a ω of 0.5 were used. The results illustrate, that the regularization sharpens the ODFs and that with increasing cone length the effect becomes more obvious. The regularized ODFs within the fiber crossing area clearly show the expected bi-directional anisotropic behavior.

We also applied the tracking algorithm, described above, to the regularized as well as the original phantom data. Fig. 3 shows the streamlines which were generated by usage of two seedboxes. Tracking through the crossing region fails due to partial voluming (left picture). After regularization with $\alpha = 30°$, $l = 2$ voxels and $\omega = 0.25$ the results are much better. Note, that smoothing with a relatively small voxel neighborhood is obviously sufficient to substantially enhance tracking results.

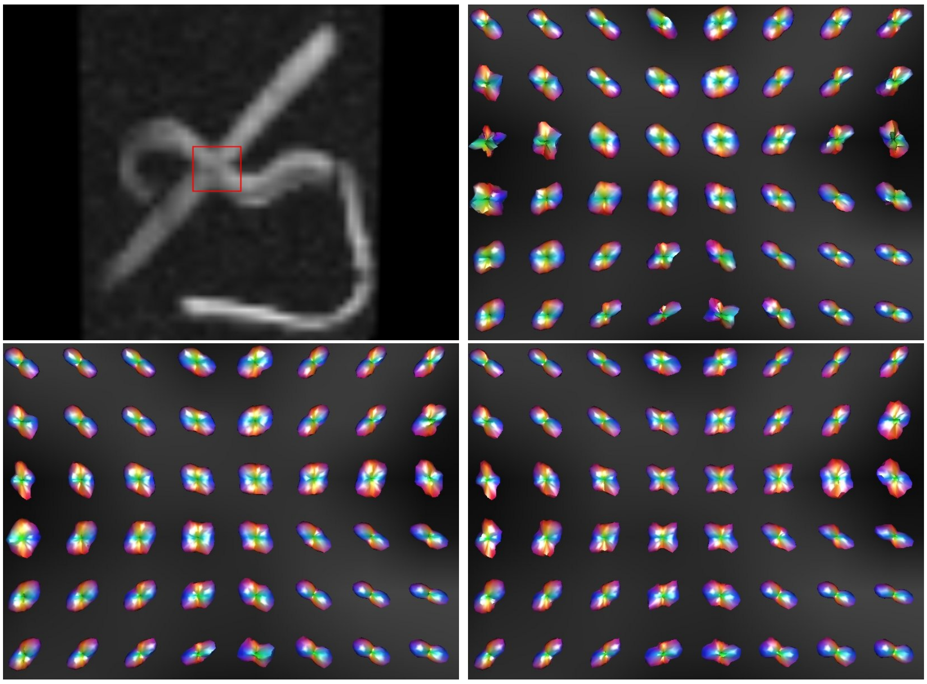

Fig. 2. Regularization impact on the shape of the ODFs in crossing area of the phantom

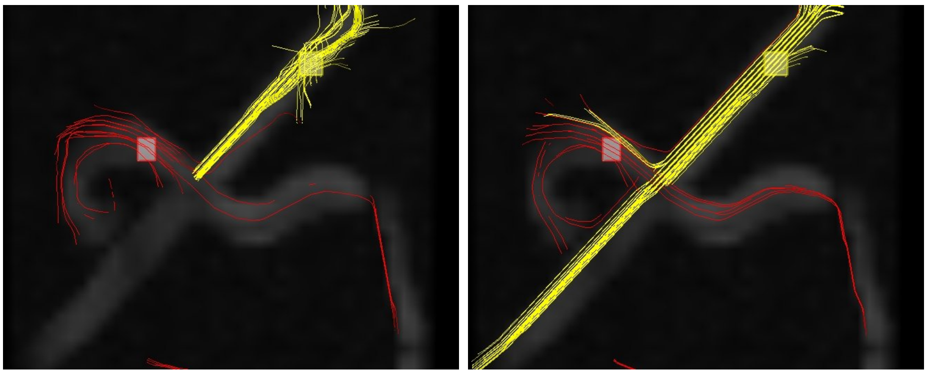

Fig. 3. Tracking result from phantom study with original ODFs (left) and after regularization (right)

Furthermore, we applied our method to data from a patient study, acquired on a 3 Tesla Trio scanner (Siemens, Erlangen) with an isotropic resolution of 2.0 mm, 126 gradient directions and 56 slices. Each 10 diffusion measurements were followed by a non-diffusion measurement, which was used to estimate the rotation matrices of a head motion correction procedure. Furthermore, an eddy current correction was performed.

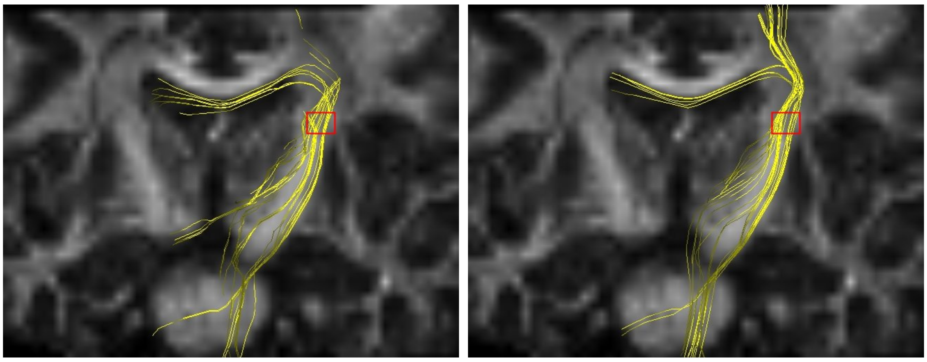

Fig. 4. Tracking result from pyramidal tract with original ODFs (left) and after regularization (right)

We focussed on the delineation of the pyramidal tract. Many studies have shown, that especially near the corpus callosum tracking of pyramidal fibers is difficult because of crossing callosal projections. This finding was confirmed by our tracking experiments, using non-regularized q-ball fields (fig. 4). After regularization with our CB-REG approach, substantially more fibers could be tracked through the crossing region. Again we used a relatively small voxel neighborhood for ODF de-noising: $\alpha = 30°$, $l = 2$, $\omega = 0.5$.

6 Conclusions

We have presented a new method for regularization of q-ball fields which does not depend on highly complex modeling assumptions. We use a cone-beam strategy with 3 parameters (cone opening angle α and length l, weight of utmost sample ω) to sharpen the ODF's shape and reduce noise. Our experiments show, that tracking fiber pathways through crossing regions benefits from the regularization of the q-ball field. Care has to be taken, not to overdo the regularization effect, e.g. by the definition of an arbitrarily large neighborhood. Artifacts might be induced, constructing wrong connections. From our studies we found, that with a neighborhood of up to two voxels and an opening angle of 25 to 35 degrees reliable results could be achieved. Currently we elaborate our strategy by incorporating anisotropy data (GFA values) into the smoothing procedure. By this we plan to reduce the erroneous influence of neighboring isotropic voxels on ODFs representing regions at fascicle borders.

Acknowledgements

We would like to thank Jennifer Campbell of the McConnell Brain Imaging Center, Montreal Neurological Institute, McGill University, for providing the phantom data, we used in our experiments.

References

1. Tuch, D.S.: Q-ball imaging. Magn. Reson. Med. 52(6), 1358–1372 (2004)
2. Parker, G.J.M., Haroon, H.A., Wheeler-Kingshott, C.A.M.: A framework for a streamline-based probabilistic index of connectivity (PICo) using a structural interpretation of mri diffusion measurements. J. Magn. Reson. Imaging 18(2), 242–254 (2003)
3. Lazar, M., Alexander, A.L.: Bootstrap white matter tractography (BOOT-TRAC). Neuroimage 24(2), 524–532 (2005)
4. Behrens, T.E.J., Berg, H.J., Jbabdi, S., Rushworth, M.F.S., Woolrich, M.W.: Probabilistic diffusion tractography with multiple fibre orientations: What can we gain? Neuroimage 34(1), 144–155 (2007)
5. Zalesky, A.: DT-MRI fiber tracking: a shortest paths approach. IEEE Trans. Med. Imaging 27(10), 1458–1471 (2008)
6. Parker, G.J., Schnabel, J.A., Symms, M.R., Werring, D.J., Barker, G.J.: Nonlinear smoothing for reduction of systematic and random errors in diffusion tensor imaging. J. Magn. Reson. Imaging 11(6), 702–710 (2000)
7. Martin-Fernandez, M., Muñoz-Moreno, E., Cammoun, L., Thiran, J.P., Westin, C.F., Alberola-López, C.: Sequential anisotropic multichannel wiener filtering with rician bias correction applied to 3d regularization of DWI data. Med. Image Anal. 13(1), 19–35 (2009)
8. Wang, Z., Vemuri, B.C., Chen, Y., Mareci, T.H.: A constrained variational principle for direct estimation and smoothing of the diffusion tensor field from complex DWI. IEEE Trans. Med. Imaging 23(8), 930–939 (2004)
9. Poupon, C., Clark, C.A., Frouin, V., Régis, J., Bloch, I., Bihan, D.L., Mangin, J.: Regularization of diffusion-based direction maps for the tracking of brain white matter fascicles. Neuroimage 12(2), 184–195 (2000)
10. Coulon, O., Alexander, D.C., Arridge, S.: Diffusion tensor magnetic resonance image regularization. Med. Image Anal. 8(1), 47–67 (2004)
11. Savadjiev, P., Campbell, J.S.W., Pike, G.B., Siddiqi, K.: 3D curve inference for diffusion MRI regularization. In: Int. Conf. on Med. Image Comput Assist Interv., vol. 8(Pt 1), pp. 123–130 (2005)
12. Jonasson, L., Bresson, X., Thiran, J.P., Wedeen, V.J., Hagmann, P.: Representing diffusion MRI in 5-D simplifies regularization and segmentation of white matter tracts. IEEE Trans. Med. Imaging 26(11), 1547–1554 (2007)
13. Descoteaux, M., Angelino, E., Fitzgibbons, S., Deriche, R.: Regularized, fast, and robust analytical q-ball imaging. Magn. Reson. Med. 58(3), 497–510 (2007)
14. Descoteaux, M., Deriche, R., Knösche, T.R., Anwander, A.: Deterministic and probabilistic tractography based on complex fibre orientation distributions. IEEE Trans. Med. Imaging 28(2), 269–286 (2009)
15. Perona, P., Malik, J.: Scale-space and edge detection using anisotropic diffusion. IEEE Transactions on Pattern Analysis and Machine Intelligence 12, 629–639 (1990)
16. Mori, S., Crain, B.J., Chacko, V.P., van Zijl, P.C.: Three-dimensional tracking of axonal projections in the brain by magnetic resonance imaging. Ann. Neurol. 45(2), 265–269 (1999)

17. Lazar, M., Weinstein, D.M., Tsuruda, J.S., Hasan, K.M., Arfanakis, K., Meyerand, M.E., Badie, B., Rowley, H.A., Haughton, V., Field, A., Alexander, A.L.: White matter tractography using diffusion tensor deflection. Hum. Brain Mapp. 18(4), 306–321 (2003)
18. Ehricke, H.H., Klose, U., Grodd, W.: Visualizing MR diffusion tensor fields by dynamic fiber tracking and uncertainty mapping. Computers & Graphics 30(2), 255–264 (2006)
19. Behrens, T.E.J., Woolrich, M.W., Jenkinson, M., Johansen-Berg, H., Nunes, R.G., Clare, S., Matthews, P.M., Brady, J.M., Smith, S.M.: Characterization and propagation of uncertainty in diffusion-weighted MR imaging. Magn. Reson. Med. 50(5), 1077–1088 (2003)
20. Perrin, M., Poupon, C., Cointepas, Y., Rieul, B., Golestani, N., Pallier, C., Rivière, D., Constantinesco, A., Bihan, D.L., Mangin, J.F.: Fiber tracking in q-ball fields using regularized particle trajectories. Inf. Process Med. Imaging 19, 52–63 (2005)
21. Campbell, J.S.W., Siddiqi, K., Rymar, V.V., Sadikot, A.F., Pike, G.B.: Flow-based fiber tracking with diffusion tensor and q-ball data: validation and comparison to principal diffusion direction techniques. Neuroimage 27(4), 725–736 (2005)